Scientific Research Publishing

Open Journal of Veterinary Medicine, 2026, 16(11), 219-236
https://www.scirp.org/journal/ojvm
ISSN Online: 2165-3364
ISSN Print: 2165-3356

Contribution to the Histological and Topographical Study of the Central Nervous System (CNS) of the Common Vampire Bat *Desmodus rotundus*

Saulo Valencia-Corona[1], Armando Zepeda-Bastida[2], Rodrigo Salomón Hernández-Aco[1], José Luis Hernández-Guzmán[3], María Guadalupe Ramírez-Muñoz[1*], Juan Ocampo-López[1*]

[1]Laboratorio de Histología e Histopatología del Área Académica de Medicina Veterinaria y Zootecnia del Instituto de Ciencias Agropecuarias de la Universidad Autónoma del Estado de Hidalgo (UAEH), Santiago Tulantepec, México
[2]Laboratorio de Bioquímica y Biología Celular y Molecular del Área Académica de Medicina Veterinaria y Zootecnia del Instituto de Ciencias Agropecuarias de la Universidad Autónoma del Estado de Hidalgo (UAEH), Santiago Tulantepec, México
[3]División de Ciencias del Medio Ambiente de la Universidad Intercultural del Estado de Hidalgo, Tenango de Doria, México
Email: *jocampo@uaeh.edu.mx, *maria_ramirez9614@uaeh.edu.mx

How to cite this paper: Valencia-Corona, S., Zepeda-Bastida, A., Hernández-Aco, R.S., Hernández-Guzmán, J.L., Ramírez-Muñoz, M.G. and Ocampo-López, J. (2026) Contribution to the Histological and Topographical Study of the Central Nervous System (CNS) of the Common Vampire Bat *Desmodus rotundus*. *Open Journal of Veterinary Medicine*, **16**, 219-236.
https://doi.org/10.4236/ojvm.2026.1611016

Received: October 9, 2026
Accepted: November 21, 2026
Published: November 24, 2026

Copyright © 2026 by author(s) and Scientific Research Publishing Inc.
This work is licensed under the Creative Commons Attribution International License (CC BY 4.0).
http://creativecommons.org/licenses/by/4.0/

Open Access

Abstract

Desmodus rotundus is an important reservoir of the rabies virus in Latin America; however, information regarding its central nervous system (CNS) remains limited. The objective of this study was to describe the main neuroanatomical structures of the brain and spinal cord of this species. Samples from three male specimens were processed using Hematoxylin-Eosin (H&E) staining and the combined Luxol Fast Blue-Hematoxylin-Eosin (LFB-H&E) staining technique. The main findings included an extensive neocortical region, identifiable olfactory structures, and the characteristic trilaminar organization of the cerebellum. Furthermore, analysis of the cervical, thoracic, and lumbar segments of the spinal cord allowed visualization of the distribution of gray and white matter, facilitating the identification of nerve tracts. These findings provide a practical histological and topographical reference for the neuroanatomical identification of *Desmodus rotundus* and facilitate comparisons with previously published anatomical descriptions, contributing to future research on this species.

Keywords

Histology, Vampire Bat, Brain, Spinal Cord, Nervous System Topography

1. Introduction

Bats have been on Earth for more than 50 million years; around 1500 species are distributed across all continents, making them the second-largest order of mammals, after rodents, which comprise over 2600 species. They play vital ecological roles, such as controlling insect pests, pollinating plants, and dispersing seeds within ecosystems [1] [2].

The order Chiroptera (from the Greek *cheir*, "hand," and *pteron*, "wing") is divided into two suborders: *Yinpterochiroptera*, which includes both echolocating families (superfamily *Rhinolophoidea*) and frugivorous/nectarivorous bats of the family *Pteropodidae*—the latter of which lack laryngeal echolocation or employ alternative, non-laryngeal mechanisms—and *Yangochiroptera*, which encompasses all other families of microchiropterans, including the family *Phyllostomidae* [3]-[5]. This suborder includes the only three hematophagous (blood-feeding) bat species (*Desmodus rotundus*, *Diphylla ecaudata*, and *Diaemus youngi*), all of which belong to the family *Phyllostomidae* and are found exclusively in Mexico, Central America, and South America [1] [2].

Within this group of hematophagous bats, *Desmodus rotundus* which weighs between 25 g and 40 g in adulthood [6], is notable for its close interaction with both domestic and wild animals; it serves as the primary reservoir and vector for the rabies virus. Furthermore, it has been linked to various zoonotic pathogens that cause diseases such as leptospirosis, bartonellosis, toxoplasmosis, Chagas disease, and coronavirus infections, increasing scientific interest in understanding its anatomy, biology, and physiology [7]-[9].

The central nervous system (CNS) of bats integrates information, processes it, and coordinates survival-related responses such as prey localization, spatial orientation, echolocation, and complex social behaviors, suggesting a specialized neuroanatomy. However, information regarding their CNS is scarce compared to that available for other animals [6] [10].

This study aims to provide a histological and topographical description of the CNS of *Desmodus rotundus* by identifying key encephalic and spinal cord structures, thereby contributing to neuroanatomical knowledge of this species, which is of great ecological and epidemiological significance.

2. Materials and Methods

2.1. Biological Sample Collection

Samples were obtained from 3 study subjects (3 adult males with an average weight of 30 g and a mean wingspan of 40 cm, which were captured in the municipalities of Huehuetla and Atotonilco el Grande, in the state of Hidalgo, Mexico). The study subjects were obtained through support and prevention programs—implemented by the State Government—for the capture of bats that transmit the rabies virus, as part of the "National Campaign for the Prevention and Control of Rabies in Cattle and Livestock Species" (NOM-067-ZOO-2007). Subsequently, the animals were euthanized using ketamine (5 mg/kg), medetomidine hydrochloride

(0.05 mg/kg), and 0.1% sodium pentobarbital (administered intrahepatically at a dose of 60 mg/kg) [11] [12]. Once the irreversible cessation of vital functions was verified, evidenced by the absence of a heartbeat, pulse, and respiratory movements, the loss of ocular and corneal reflexes, and the presence of muscular flaccidity [12], the brain and vertebral column were carefully dissected. These tissues were then fixed for 24 hours in a 3.7% aqueous, phosphate-buffered formaldehyde solution [13] to allow for the histological examination of the three selected specimens.

The protocol for this project was submitted to the Institutional Ethics Committee for the Care and Use of Laboratory Animals at the Autonomous University of the State of Hidalgo and was approved under reference number CICUAL-V-I/017/2023 (**Figure 1**).

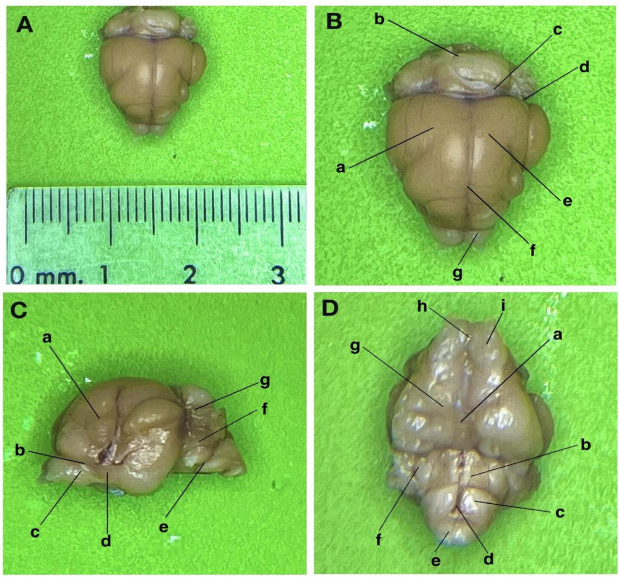

Figure 1. Brain of the common vampire bat (*Desmodus rotundus*). (A) General dorsal view of the brain with scale bar. (B) Dorsal view: left cerebral hemisphere (a), cerebellar vermis (b), cerebellar hemisphere (c), transverse fissure (d), right cerebral hemisphere (e), longitudinal fissure (f), and olfactory bulb (g). (C) Lateral view: left cerebral hemisphere (a), rhinal sulcus (b), olfactory bulb (c), olfactory tract (d), pons (e), left cerebellar hemisphere (f), and cerebellar vermis (g). (D) Ventral view: mammillary body (a), pons (b), trapezoid body (c), pyramidal tract (d), spinal cord (e), right cerebellar hemisphere (f), piriform lobe (g), olfactory bulb (h), and olfactory tract (i).

2.2. Anatomical Dissection and Histological Processing

Dissection was performed to extract the brain, which was subsequently examined in various anatomical planes to describe its external morphology. Transverse sections were then made in a rostrocaudal direction—labeled as sections I - IV—allowing for the observation of the general anatomical arrangement of the primary brain regions at each level. The brains, measuring approximately 1.3 cm in length and 1 cm in width, were examined and divided transversely into four rostrocaudal

levels, spaced at intervals of 0.3 to 0.4 cm: (I) rostral telencephalic (frontal lobe, olfactory structures); (II) telencephalic-diencephalic (neocortex, thalamus, and hypothalamus); (III) caudal telencephalic-mesencephalic (oculomotor nucleus, optic stratum); and (IV) rhombencephalic (cerebellum, pons, and medulla oblongata) (**Figure 2**). These structures served as anatomical landmarks for characterizing the levels examined.



Figure 2. Transverse sections of the *Desmodus rotundus* brain. Brain segments sectioned along the rostrocaudal axis, identified as I - IV.

Once the vertebral column had been dissected, and in order to preserve the integrity of the spinal cord, the samples were processed while still contained within the bony structures, following decalcification with an equal-parts mixture of 8% hydrochloric acid and 8% formic acid—a solution that was replaced daily for three days [13]. Subsequently, the column was divided transversely in a craniocaudal direction into seven clearly defined anatomical regions: (I) cervical, (II - III) thoracic, (IV) thoracolumbar transition, (V) lumbar, (VI) lumbosacral transition, and (VII) sacral (**Figure 3**). These divisions correspond to vertebral levels and do not necessarily equate to the corresponding spinal cord segments. This organization provided a systematic frame of reference for the morphological analysis and histological study of each vertebral segment.



Figure 3. Vertebral column of the common vampire bat (*Desmodus rotundus*). (A) Dorsal view of the complete vertebral column. (B) Vertebral column segmented for histological processing into seven regions arranged in a craniocaudal direction: cervical vertebrae (I), first section of thoracic vertebrae (II), second section of thoracic vertebrae (III), cervicothoracic transition (IV), first section of lumbar vertebrae (V), lumbosacral transition (VI), and sacrum (VII).

Sections of the brain and spinal cord were placed in histology cassettes for processing by paraffin embedding [13]; briefly, an automated Microm processor (model STP120) was used for washing, dehydration, clearing, and infiltration with histological-grade paraffin. The resulting samples were embedded in histological-grade paraffin blocks, sectioned at 6 - 8 μm using a Leica manual rotary microtome (model RM2125RT), mounted on slides using a Premiere flotation bath, and stored for staining. Histological sections were selected that allowed for a clear and complete observation of the anatomical structures at each level under study. Priority was given to sections that were intact, clean, well-preserved, and free from significant morphological alterations resulting from the processing procedure. For each anatomical level, the two highest-quality sections were chosen, with no fixed interval established between them.

2.3. Histological Staining

To evaluate the quality of the histological sections and identify the main structures in each central nervous system section, hematoxylin-eosin (H-E) staining was used to verify adequate morphological preservation and identify the histological components of each section. Subsequently, Luxol Fast Blue followed by hematoxylin-eosin staining was used, enabling clear differentiation between gray and white matter and identification of key nervous tissue elements: neuronal cell bodies, neuroglial nuclei, and myelinated nerve fibers. This combined technique enabled identification of major neuroanatomical structures and served as the basis for creating topographic maps of the brain and spinal cord of *Desmodus rotundus* [13] [14].

2.4. Microscopic Observation, Image Acquisition, and Analysis

We analyzed hematoxylin-eosin (H-E) sections and Luxol Fast Blue/hematoxylin-eosin (H-E) sections by bright-field light microscopy using an Olympus CX31 microscope at 40×, 100×, and 400× magnification to identify key structures in the brain and spinal cord of *Desmodus rotundus*. We used H-E-stained sections to assess tissue morphological preservation and document histological findings in TIFF-format images captured with an Olympus BX41 bright-field compound microscope equipped with an EvolutionPro digital camera (MediaCybernetics) and ImagePro Express v. 6.0 software (MediaCybernetics). Additionally, sections stained with the combined Luxol Fast Blue/hematoxylin-eosin technique were used for the topographic analysis of the central nervous system; these preparations were examined under an Upsehkraft stereomicroscope and photographed using an iPhone 13 camera (12 MP, f/1.6 aperture). The resulting images were processed using the generative artificial intelligence tool ChatGPT (OpenAI), specifically the GPT-4o Image Generation model, available as of November 2025. The instructions provided were to preserve the original structure, texture, and coloration of the tissue; remove background tones and imperfections; establish a uniform white background; and standardize the images into a square format (1:1) at high resolution.

Verification was conducted through a qualitative visual comparison between the original and processed images, assessing the similarity of tissue contours, anatomical boundaries, and observable morphological characteristics. Finally, based on the interpretation of the histological preparations and processed images, topographic maps of the brain and spinal cord were created using an Apple Pencil (2nd generation) and an iPad Pro M2 (6th generation) with the Goodnotes app (Goodnotes Ltd.), allowing for the representation and identification of the main structures observed at each anatomical level [14].

3. Results

3.1. Anatomy

The general dorsal view (**Figure 1(A)**) shows the brain's external conformation, with a reference scale. In the same orientation (**Figure 1(B)**), both cerebral hemispheres, separated by the longitudinal fissure, and the olfactory bulb in the rostral region are visible. Toward the caudal portion, the cerebellum is visible; it is separated from the cerebral hemispheres by the transverse fissure and consists of the vermis and the cerebellar hemispheres. In the lateral view (**Figure 1(C)**), the left cerebral hemisphere, rhinal sulcus, and olfactory bulb and tract are identified; additionally, the pons, left cerebellar hemisphere, and cerebellar vermis are observed in the caudal region. In the ventral view (**Figure 1(D)**), structures such as the mammillary body, pons, trapezoid body, pyramidal tract, and spinal cord can be distinguished. The right cerebellar hemisphere, piriform lobe, and olfactory bulb and tract are also recognizable, allowing a comprehensive description of the macroscopic organization of the *Desmodus rotundus* brain.

3.2. Histology

Based on observations and digitization of serial transverse histological sections of the brain and spinal cord of *Desmodus rotundus*, we identified and morphologically described each structural component and the organization of the central nervous system. Representative images are shown in **Figure 4**: The surface of the medulla oblongata is observed, in which the arachnoid and pia mater meninges, the tectospinal and ventral spinocerebellar tracts, the inferior olivary nuclei, the reticular substance, and the dorsal accessory olivary nucleus are identified (**Figure 4(A)**). A cerebral gray matter nucleus is shown, in which myelinated nerve fibers, large neuronal cell bodies, and blood vessels are identified (**Figure 4(B)**). The three zones of the cerebellar cortex are displayed: the molecular zone, the layer of pyriform neurons, and the granular zone (**Figure 4(C)**). Finally, a spinal cord section is presented, showing the ventral median sulcus, the external white matter, and the internal gray matter (**Figure 4(D)**).

3.3. Topographic Anatomy of the Central Nervous System

In **Figure 5**, corresponding to section I of the *Desmodus rotundus* brain, the neocortex is visible. It occupies a large portion of the section, followed by the cingu-

lum, the forceps minor of the corpus callosum, the genu of the corpus callosum, the frontal lobe, and the putamen. Posterior to this, the olfactory area is observed, where the accessory olfactory bulb, the olfactory ventricle, the main olfactory bulb, and the olfactory nerve are also visible.

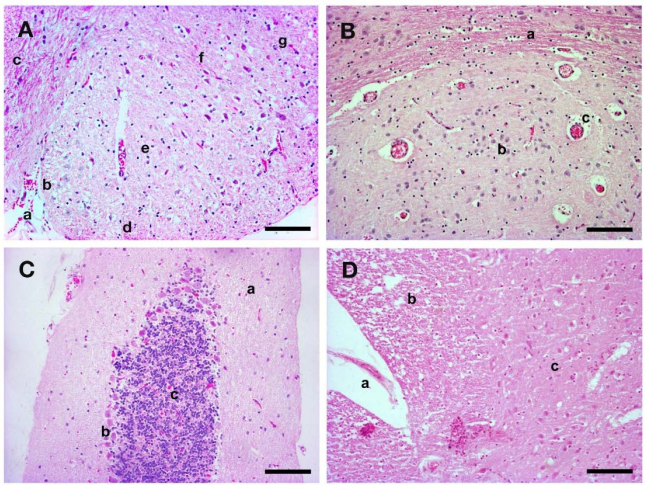

Figure 4. Brain and spinal cord of *Desmodus rotundus* (H-E stain). In **Figure 4(A)**, the surface of the medulla oblongata is shown, where the arachnoid (a), pia mater (b), tectospinal tract (c), ventral spinocerebellar tract (d), inferior olivary nuclei (e), reticular substance (f), and dorsal accessory olivary nucleus (g) can be observed. **Figure 4(B)** shows a gray matter nucleus of the brain, identifying myelinated nerve fibers (a), large neuronal cell bodies (b), and blood vessels (c). **Figure 4(C)** shows a section of the cerebellar cortex, identifying the three known layers: the molecular layer (a), the piriform neurons layer (b), and the granular layer (c). **Figure 4(D)** shows a cross-section of the spinal cord, displaying the ventral median fissure (a), the outer white matter (b), and the inner gray matter (c).

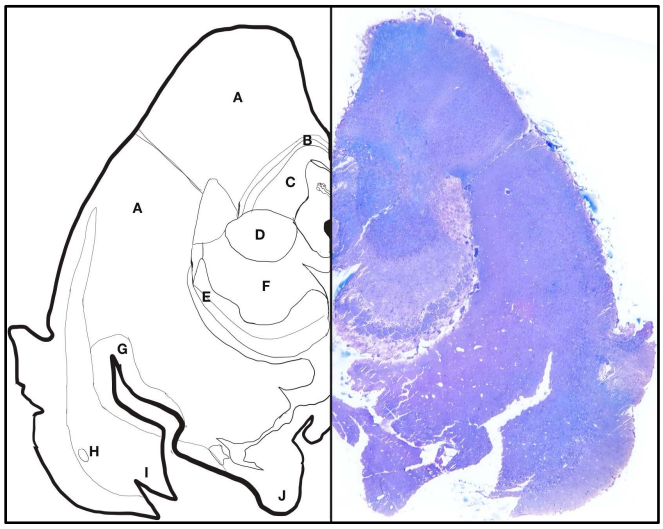

Figure 5. Cross-section corresponding to section I of the *Desmodus rotundus* brain, stained using the combined Luxol Fast Blue-Hematoxylin-Eosin technique: neocortex (A), cingulum (B), forceps minor of the corpus callosum (C), genu of the corpus callosum (D), frontal lobe (E), putamen (F), accessory olfactory bulb (G), olfactory ventricle (H), main olfactory bulb (I), and olfactory nerve (J).

Figure 6 shows section II of the *Desmodus rotundus* brain; visible are the neocortex, which spans much of the section, the zonal stratum, the brachium of the superior colliculus, the dentate nucleus, and the medial and lateral geniculate bodies. Also evident are the medial lemniscus, the brachium of the inferior colliculus, and the zona incerta, along with the substantia nigra, the cerebral peduncle, and the hypothalamus. Furthermore, the following structures are identified: the mammillothalamic tract, the mammillary body, the periventricular gray matter, the peduncle of the mammillary body, the mammillotegmental tract, the third ventricle, the red nucleus, the central tegmental tract, the posterior thalamic nucleus, the interstitial nucleus, the superior colliculus, the lemniscal stratum, the optic stratum, the central gray matter, the cerebral aqueduct, and the commissure of the superior colliculus.

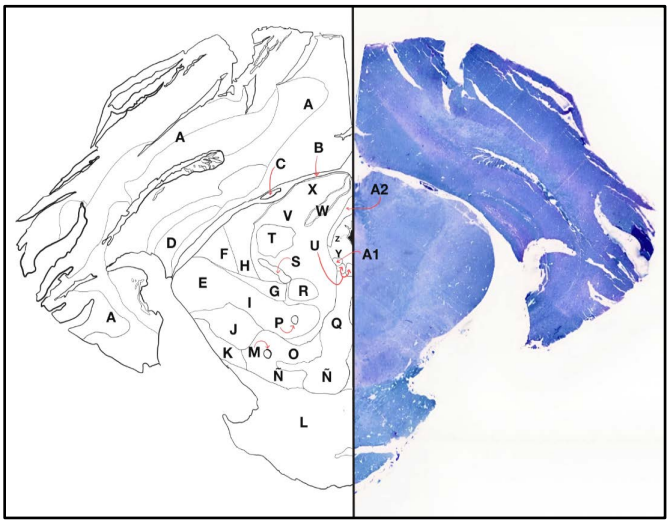

Figure 6. Transverse section corresponding to section II of the *Desmodus rotundus* brain, stained using the combined Luxol Fast Blue-Hematoxylin-Eosin technique: neocortex (A), zonal stratum (B), brachium of the superior colliculus (C), dentate nucleus (D), medial geniculate body (E), lateral geniculate body (F), medial lemniscus (G), brachium of the inferior colliculus (H), zona incerta (I), substantia nigra (J), cerebral peduncle (K), hypothalamus (L), mammillothalamic tract (M), mammillary body (N), periventricular gray matter (Ñ), peduncle of the mammillary body (O), mammillotegmental tract (P), third ventricle (Q), red nucleus (R), central tegmental tract (S), posterior thalamic nucleus (T), interstitial nucleus (U), superior colliculus (V), lemniscal stratum (W), optic stratum (X), central gray matter (Y), cerebral aqueduct (Z), interstitial nucleus (A1), and commissure of the superior colliculus (A2).

In Figure 7, corresponding to section III of the *Desmodus rotundus* brain, the neocortex again occupies a large area. Additionally, the medial geniculate body, the brachium of the inferior colliculus, the commissure of the superior colliculus, the substantia nigra, and the superior colliculus are identified. Furthermore, structures related to the visual pathway and ocular motility such as the optic stratum, the oculomotor nerve, and the oculomotor nucleus can be distinguished. Also observed are the lemniscal stratum, the central gray matter, the dorsal loop of the

lateral lemniscus, the decussation of the tectospinal tract, the central tegmental tract, the rubrospinal tract, the medial longitudinal fasciculus, the medial lemniscus, the decussation of the middle cerebellar peduncle, the cerebral peduncle, the interpeduncular nucleus, and the pons.

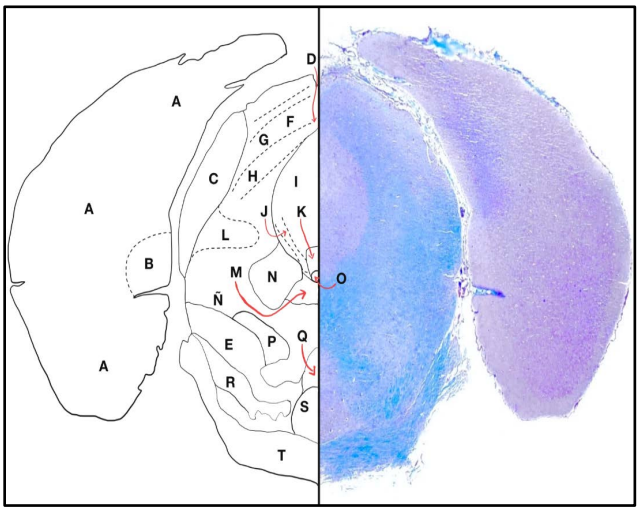

Figure 7. Transverse section corresponding to section III of the *Desmodus rotundus* brain, stained using the combined Luxol Fast Blue-Hematoxylin-Eosin technique: neocortex (A), medial geniculate body (B), brachium of the inferior colliculus (C), commissure of the superior colliculus (D), substantia nigra (E), superior colliculus (F), optic stratum (G), lemniscal stratum (H), central gray matter (I), oculomotor nerve (J), oculomotor nucleus (K), dorsal loop of the lateral lemniscus (L), decussation of the tectospinal tract (M), central tegmental tract (N), rubrospinal tract (Ñ), medial longitudinal fasciculus (O), medial lemniscus (P), decussation of the middle cerebral peduncle (Q), cerebral peduncle (R), interpeduncular nucleus (S), and pons (T).

Finally, **Figure 8**, corresponding to section IV of the *Desmodus rotundus* brain, identifies various structures associated with the brainstem and cerebellum. Among these, the trapezoid body, nucleus of the trapezoid body, median raphe nucleus, medial lemniscus, tectospinal tract, and nucleus of the lateral lemniscus are observed. Likewise, the granular and molecular layers are distinguishable; these form part of the cerebellum, which is highly prominent in this section because of its more caudal location within the brain series. Also identified are the rubrospinal tract, lateral lemniscus, inferior colliculus, reticular formation, central gray matter, medial longitudinal fasciculus, dorsal raphe nucleus, dorsal tegmental nuclei, pons, and median eminence.

The results of the topographical study of the spinal cord of *Desmodus rotundus* are presented below. **Figures 9-11** show transverse sections of the cervical, thoracic, and lumbar regions, respectively. Various neuroanatomical structures were identified, most notably the gracile and cuneate fasciculi, the corticospinal and rubrospinal tracts, and several nerve conduction pathways. In the thoracic and lumbar regions, the spinal funiculi, the central canal, various laminae of the gray matter, and groups of motor neurons were observed. Furthermore, specific struc-

tures characteristic of each anatomical level was identified, which enabled a description of the organization and topographical distribution of the gray and white matter in the regions studied.

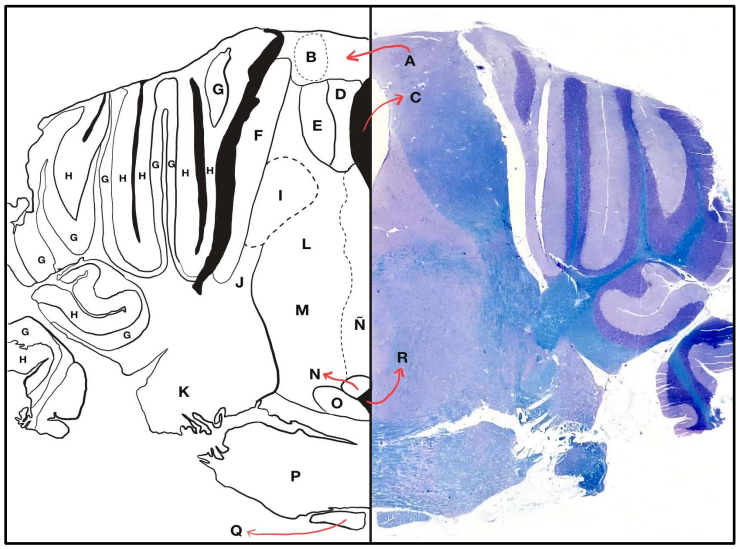

Figure 8. Cross-section corresponding to section IV of the *Desmodus rotundus* brain, stained using the combined Luxol Fast Blue-Hematoxylin-Eosin technique: trapezoid body (A), nucleus of the trapezoid body (B), median raphe nucleus (C), medial lemniscus (D), tectospinal tract (E), nucleus of the lateral lemniscus (F), granular zone (G), molecular zone (H), rubrospinal tract (I), lateral lemniscus (J), inferior colliculus (K), reticular formation (L), central gray matter (M), medial longitudinal fasciculus (N), dorsal raphe nucleus (Ñ), dorsal tegmental nuclei (O), pons (P), and median eminence (Q).

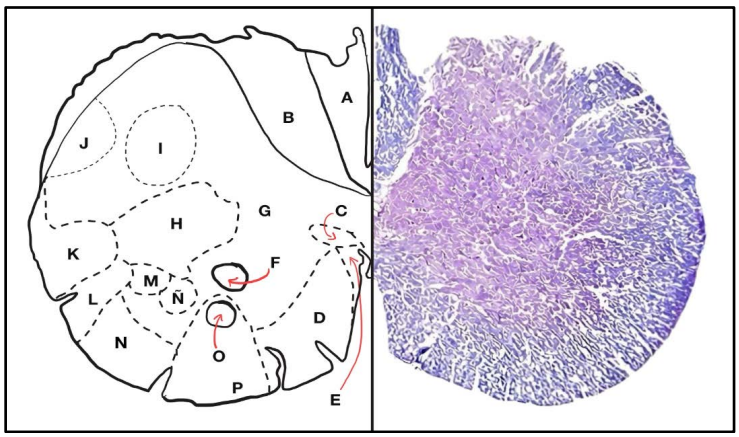

Figure 9. Cross-section corresponding to section I of the cervical spinal cord of *Desmodus rotundus*, stained using the combined Luxol Fast Blue-Hematoxylin-Eosin technique: gracile fasciculus (A), cuneate fasciculus (B), medial longitudinal fasciculus (C), tectospinal tract (D), ventral corticospinal tract (E), dorsal nucleus of origin of the accessory nerve (F), reticular formation (G), lateral corticospinal (pyramidal) tract (H), nucleus of the spinal tract of the trigeminal nerve (I), spinal tract of the trigeminal nerve (J), dorsal spinocerebellar tract (K), lateral vestibulospinal tract (L), lateral spinothalamic tract (M), spinoolivary tract (N), rubrospinal tract (Ñ), ventral nucleus of origin of the accessory nerve (O), and lateral vestibulospinal tract (P).

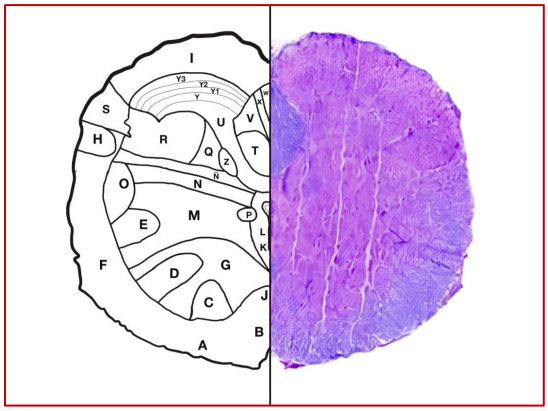

Figure 10. Cross-section corresponding to section II of the thoracic spinal cord of *Desmodus rotundus*, stained using the combined Luxol Fast Blue-Hematoxylin-Eosin technique: ventral funiculus (A), ventral median fissure (B), axial muscle motoneurons of lamina 9 (C), intercostal muscle motoneurons of lamina 9 (D), manus motoneurons of lamina 9 (E), lateral funiculus (F), lamina 8 of the spinal gray (G), rubrospinal tract (H), dorsolateral fasciculus (Lissauer) (I), ventral white commissure (J), lamina 10 of the spinal gray (K), central canal (L), lamina 7 of the spinal gray (M), intercalated nucleus (N), lamina 7 of the spinal gray (Ñ), intermediolateral column (O), intermediomedial column (P), medial part of lamina 5 of the spinal gray (Q), lateral part of lamina 5 of the spinal gray (R), lateral spinal nucleus (S), dorsal corticospinal tract (T), lamina 4 of the spinal gray (U), cuneate fasciculus (V), gracile fasciculus (W), postsynaptic dorsal column pathway (X), lamina 3 of the spinal gray (Y), inner part of lamina 2 of the spinal gray (Y1), outer part of lamina 2 of the spinal gray (Y2), lamina 1 of the spinal gray (Y3), and dorsal nucleus (Clarke) (Z).

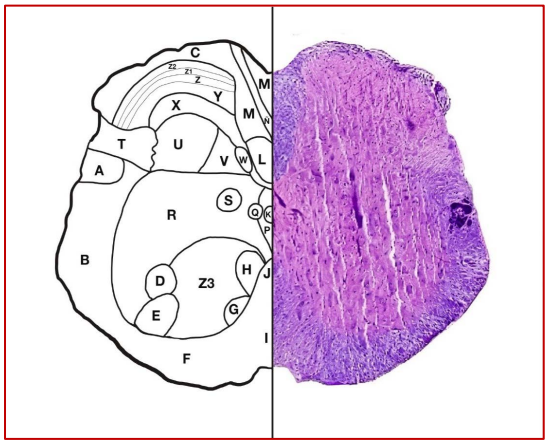

Figure 11. Cross-section corresponding to section V of the lumbar spinal cord of *Desmodus rotundus*, stained using the combined Luxol Fast Blue-Hematoxylin-Eosin technique: rubrospinal tract (A), lateral funiculus (B), dorsolateral fasciculus of Lissauer (C), adductor motoneurons of lamina IX (D), quadriceps motoneurons of lamina IX (E), ventral funiculus (F), psoas motoneurons of lamina IX (G), axial muscle motoneurons of lamina IX (H), ventral median fissure (I), ventral white commissure (J), central canal (K), dorsal corticospinal tract (L), gracile fasciculus (M), postsynaptic dorsal column pathway (Ñ), lamina X of the spinal gray matter (P), intermediomedial column (Q), lamina VII of the spinal gray matter (R), lumbar precerebellar nucleus (S), lateral spinal nucleus (T), lateral part of lamina V (U), medial part of lamina V (V), dorsal nucleus of Clarke (W), lamina IV (X), lamina III (Y), inner part of lamina II (Z), outer part of lamina II (Z1), lamina I (Z2), and lamina VIII (Z3).

4. Discussion

This study describes the histological and topographical organization of the central nervous system of *Desmodus rotundus* by analyzing selected sections of the brain and the cervical, thoracic, and lumbar segments of the spinal cord. Based on these sections, we identified key morphological structures and created topographical maps to illustrate their locations clearly. The general organization of the nervous system follows a structural pattern conserved across vertebrates, in which the neural tube is organized into longitudinal and transverse units that contribute to the establishment of the main regions of the central nervous system: the forebrain (prosencephalon), midbrain (mesencephalon), and hindbrain (rhombencephalon). This conserved pattern provides a common basis for interspecies comparison. At the same time, variations in the development and differentiation of these regions give rise to distinct neuroanatomical configurations in size, shape, and distribution across vertebrate species [15]. During embryonic development, various regions such as the neural tube, neural crest, and primary brain vesicles (forebrain, midbrain, and hindbrain) give rise to the neurons, supporting cells, and structures that form the brain and spinal cord [16] [17]. Understanding this embryological process shows that the adult organization results from the orderly formation of its regions, which helps interpret the structures in the analyzed sections.

Bhatnagar (2008) [18] pioneered the description of the tissue cytoarchitecture of the *Desmodus rotundus* brain. In this context, it was deemed appropriate to review the information considering improvements in staining techniques and the availability of generative AI tools. Comparisons with this atlas and other histological studies on bats enabled the identification of the locations of cortical regions, nuclei, tracts, and brainstem structures [19]. We also included a previously undocumented microscopic topographic description of the *Desmodus rotundus* spinal cord.

One of the clearest findings was the neocortex's extensive size, consistent with previous descriptions of *Desmodus rotundus* [18]. Developmentally, neocortical expansion may be linked to increased neuronal production and a prolonged period of neuronal formation. According to the scientific literature, it can be hypothesized that, in functional terms, an increase in neocortical surface area and integration enhances the capacity for information integration; this, in turn, facilitates greater behavioral and adaptive specialization in response to the demands of the ecological niche occupied by this bat species [18] [20]. This region integrates sensory information and is generally associated with orientation, social interaction, feeding, and environmental adaptation [6]. Other studies on bats have also described adaptations in auditory processing [21] [22], the role of spatial memory, and the coordination of sensory information and movement during navigation [20]. In *Desmodus rotundus*, the lateral trigeminal nucleus of the brainstem has also been identified as a potential site involved in detecting infrared stimuli [23]. Furthermore, the literature reports variations in brain antioxidant defenses associated with a hematophagous diet. Blood ingestion entails a metabolic process that

generates high levels of nitrites and nitrates, increasing oxidative stress and the risk of tissue damage. Although we did not evaluate these parameters in the present study, they provide a physiological background that helps contextualize our morphological observations. The demands of neutralizing this physiological toxicity exert selective pressure on the central nervous system, requiring strict oxidative homeostasis to preserve cytoarchitecture and resist neurodegeneration in these species [24]. Taken together, all these findings and background data demonstrate the relationship between brain organization and functions important for the orientation, environmental perception, and feeding of *Desmodus rotundus*.

The sections also showed the main olfactory bulb, accessory olfactory bulb, ventricle, and olfactory nerve. The olfactory bulb is the first brain region to process information from the nasal cavity [25]; therefore, identifying it is important in a species whose behaviors depend largely on smell and the vomeronasal system [6]. Close contacts between astrocyte processes and mitral cell dendrites have been described in this same region. Astrocyte processes that delimit mitral cell axodendritic and dendrodendritic synapses imply active synaptic modulation. This structural coupling allows astrocytes to detect neurotransmitter (glutamate) release and dynamically regulate excitability, thereby optimizing the sensory signal transmitted from olfactory nerve terminals to the brain [26] [27]. Although the present study did not directly evaluate these cellular relationships, their prior description illustrates the olfactory bulb's microscopic complexity. It complements the identification of this structure in the sections presented here.

In the caudal sections, we observed a prominent cerebellum; this structure is associated with balance, coordination, and precise control of movement [10]. These functions are essential for flight, terrestrial locomotion, and prey capture [6]. Although cerebellar size and the degree of folding vary among mammals, the fundamental features of its organization remain consistent [28]. The cerebellum consists of the vermis and cerebellar hemispheres, which are structurally organized into a cerebellar cortex (gray matter) and a cerebellar medulla (white matter). The cerebellar cortex comprises three layers arranged from the outside in: the molecular layer, the piriform neurons layer, and the granular layer. The cerebellar medulla, meanwhile, has a distinct tree-like appearance and consists of neuroglia and neuropil. Finally, the cerebellum integrates functionally and anatomically with the rest of the central nervous system via the superior, middle, and inferior cerebellar peduncles [29]. We also identified the pons, the medulla oblongata, and various tracts; these serve as important reference points for recognizing and locating different brainstem regions, as previously demonstrated in histological studies of *Desmodus rotundus* [19]. Precisely delineating these structures is vital in this species, given that the brainstem houses nuclei and tracts key to the organism's survival and adaptation. Notable among these are the lateral trigeminal nucleus, which processes facial thermoreception essential for locating blood vessels in prey, and the cochlear nucleus and inferior colliculus [23] [30], which are associated with hearing and echolocation. This region also plays a role in mo-

tor control of complex behaviors linked to the animal's hematophagous diet [23]. Although the topographic maps did not include the pineal gland, examining it allowed a more complete description of the brain, given that a deep, lobulated location, abundant vascularization, and distinctive cellular and nerve fiber characteristics have been described for this gland in *Desmodus rotundus* [31]. Because this structure was not included in the mapping, its description is complementary background information rather than a topographic finding of the present study.

The cervical, thoracic, and lumbar segments of the spinal cord showed a similar organization, with gray matter in the center and white matter surrounding it. This distribution, along with ascending and descending tracts, matches the general pattern described for the mammalian spinal cord [32] [33]. The spinal cord of *Yangochiroptera* features a butterfly-shaped central gray matter surrounding the central canal. The ventral horns contain motor neurons, while the dorsal horns house neurons associated with sensory reception. The gray matter is proportionally highly developed, far exceeding the volume of the white matter. The white matter surrounds the gray matter and consists of afferent and efferent funiculi and fascicles; however, in *Yangochiroptera*, these tracts are relatively reduced. The posterior funiculus is small and almost encircled by the dorsal horns. At the tip of the dorsal horns, a prominent gelatinous substance is present, which is related to the high sensitivity of the wing membrane. Regionally, the spinal cord displays a notable cervical enlargement (C1 - C8) associated with wing innervation. This region can account for nearly half the total length of the spinal cord and is called the "wing brain". Furthermore, because the vertebral column continues to grow after birth while the spinal cord does not, the latter appears relatively short compared with the vertebral canal [2]. Identifying this organization made it possible to recognize the general arrangement of the various spinal cord regions and to compare them across the analyzed segments. Based on the sections analyzed, the maps present the approximate locations of various fascicles, tracts, and nuclei. This topographic description provides additional information on spinal cord organization in *Desmodus rotundus*, given that specific information on this region is more limited than that available for the brain.

Methodologically, H-E staining confirmed preservation of the processed tissue and allowed recognition of general structures. However, the best differentiation between white matter myelin fibers and gray matter neuronal cell bodies was achieved by combining Luxol Fast Blue with Hematoxylin-Eosin. This technique was fundamental for identifying key neuroanatomical structures and creating topographic maps [19] [34] [35].

The topographic maps were developed as a practical resource to facilitate the identification and study of central nervous system structures in *Desmodus rotundus*. In addition to displaying deep brain structures, they provided a relatively simple way to represent the location and relationships of nuclei and tracts [36] [37]. Edited histological images and diagrams have also been proposed as useful tools for better understanding nervous system morphology [38]. Similarly, histo-

logical images and digital models have been used to represent brain organization in other bat species [29], and in *Desmodus rotundus*, these tools have enabled the mapping of hypothalamic nuclei and their relationships with adjacent structures [39]. In this regard, the maps produced in the present study can serve as a visual aid to facilitate the recognition and study of the species' central nervous system structures. The small sample size—consisting of three males—and the selective choice of anatomical sections are direct limitations that preclude the assessment of differences based on sex or population and restrict the generalizability of the results to the entire species.

5. Conclusions

This study provides a histological and topographical description of the central nervous system of *Desmodus rotundus* by integrating selected brain and spinal cord sections with orienting anatomical maps. The combined Luxol Fast Blue-Hematoxylin-Eosin staining technique improved the differentiation between gray and white matter, facilitating the visualization of the key neural structures observed.

The topographical maps produced represent the primary contribution of this work, offering a complementary visual tool for identifying encephalic and spinal regions in this species. Notable identified structures include the neocortex, components of the olfactory system, the cerebellum, brainstem structures, and spinal tracts; we determined their locations through histological observation and anatomical comparison with existing literature.

This study advances knowledge regarding the anatomy and histology of the central nervous system of *Desmodus rotundus*. It serves as a foundational reference for students, educators, and researchers interested in chiropteran neuroanatomy. It also provides a descriptive basis for future anatomical, comparative, and functional studies requiring higher resolution.

Author Contributions

Saulo Valencia-Corona: Investigation, histological processing, initial data analysis, and initial writing. Armando Zepeda-Bastida: Investigation and supervision. Rodrigo Salomón Hernández-Aco: Investigation and supervision. José Luis Hernández-Guzmán: Capture, transport and euthanasia of the bats used in this study, in accordance with the guidelines of the Official Mexican Standards NOM-067-ZOO-2007 and NOM-033-SAG/ZOO-2014. María Guadalupe Ramírez-Muñoz: Conceptualization, methodology, investigation and writing. Juan Ocampo-López: Conceptualization, methodology, investigation, supervision, writing, and overall coordination of the study. All authors reviewed and approved the final version of the manuscript.

Conflicts of Interest

The authors declare no conflicts of interest regarding the publication of this paper.

References

[1] Bat Conservation International (2024) Bats 101. https://www.batcon.org/about-bats/bats-101/

[2] Neuweiler, G. (2000) The Biology of Bats (E. Covey, Trans.). Oxford University Press.

[3] Agnarsson, I., Zambrana-Torrelio, C.M., Flores-Saldana, N.P. and May-Collado, L.J. (2011) A Time-Calibrated Species-Level Phylogeny of Bats (Chiroptera, Mammalia). *PLOS Currents*, **3**, RRN1212. https://doi.org/10.1371/currents.rrn1212

[4] Teeling, E.C., Springer, M.S., Madsen, O., Bates, P., O'Brien, S.J. and Murphy, W.J. (2005) A Molecular Phylogeny for Bats Illuminates Biogeography and the Fossil Record. *Science*, **307**, 580-584. https://doi.org/10.1126/science.1105113

[5] Tsagkogeorga, G., Parker, J., Stupka, E., Cotton, J. and Rossiter, S. (2013) Phylogenomic Analyses Elucidate the Evolutionary Relationships of Bats. *Current Biology*, **23**, 2262-2267. https://doi.org/10.1016/j.cub.2013.09.014

[6] Greenhall, A.M., Joermann, G., Schmidt, U. and Seidel, M.R. (1983) Desmodus Rotundus. *Mammalian Species*, No. 202, 1-6. https://doi.org/10.2307/3503895

[7] Brown, N. and Escobar, L.E. (2023) A Review of the Diet of the Common Vampire Bat (Desmodus Rotundus) in the Context of Anthropogenic Change. *Mammalian Biology*, **103**, 433-453. https://doi.org/10.1007/s42991-023-00358-3

[8] Brandão, P.E., Scheffer, K., Villarreal, L.Y., Achkar, S., Oliveira, R.D.N., Fahl, W.D.O., *et al*. (2008) A Coronavirus Detected in the Vampire Bat Desmodus Rotundus. *Brazilian Journal of Infectious Diseases*, **12**, 466-468. https://doi.org/10.1590/s1413-86702008000600003

[9] Anthony, S.J., Ojeda-Flores, R., Rico-Chávez, O., Navarrete-Macias, I., Zambrana-Torrelio, C.M., Rostal, M.K., *et al*. (2013) Coronaviruses in Bats from Mexico. *Journal of General Virology*, **94**, 1028-1038. https://doi.org/10.1099/vir.0.049759-0

[10] Dyce, K.M., Sack, W.O. and Wensing, C.J.G. (2010) Textbook of Veterinary Anatomy. 4th Edition, Saunders/Elsevier.

[11] Secretaría de Agricultura, Ganadería, Desarrollo Rural, Pesca y Alimentación (2015) NORMA Oficial Mexicana NOM-033-SAG/ZOO-2014, Métodos para dar muerte a los animales domésticos y silvestres. *Diario Oficial de la Federación*. https://www.dof.gob.mx/nota_detalle.php?codigo=5405210&fecha=26/08/2015

[12] Leary, S., Underwood, W., Anthony, R., Cartner, S., Grandin, T., Greenacre, C., Gwaltney-Brant, S., McCrackin, M.A., Meyer, R., Miller, D., Shearer, J. and Yanong, R. (2020) AVMA Guidelines for the Euthanasia of Animals: 2020 Edition. American Veterinary Medical Association (AVMA). https://www.avma.org/sites/default/files/2020-02/Guidelines-on-Euthanasia-2020.pdf

[13] Prophet, E., Mills, B., Arrington, J. and Sobin, L. (1995) Métodos Histotecnológicos. Instituto de Patología de las Fuerzas Armadas de los Estados Unidos de América (AFIP).

[14] Pérez Chávez, A. (2025) Estudio histológico descriptivo y topográfico del sistema nervioso central de la garza ganadera (Bubulcus ibis ibis). Tesis de Licenciatura, Universidad Autónoma del Estado de Hidalgo.

[15] Wullimann, M.F. (2016) Nervous System Architecture in Vertebrates. In: Shepherd, S.V., Ed., *The Wiley Handbook of Evolutionary Neuroscience*, Wiley, 236-278.

[16] Angevine, J.B., Bodian, D., Coulombre, A.J., Edds, M.V., Hamburger, V., Jacobson, M., *et al*. (1970) Embryonic Vertebrate Central Nervous System: Revised Terminology. *The Anatomical Record*, **166**, 257-261. https://doi.org/10.1002/ar.1091660214

[17] Keynes, R. and Lumsden, A. (1990) Segmentation and the Origin of Regional Diversity in the Vertebrate Central Nervous System. *Neuron*, **4**, 1-9. https://doi.org/10.1016/0896-6273(90)90438-l

[18] Bhatnagar, K. (2008) The Brain of the Common Vampire Bat, Desmodus Rotundus Murinus (Wagner, 1840): A Cytoarchitectural Atlas. *Brazilian Journal of Biology*, **68**, 583-599. https://doi.org/10.1590/s1519-69842008000300017

[19] Landoni González, M.E. and Larrosa Moreira, F. (2018) Caracterización anatómica e histológica del sistema nervioso central de ejemplares de murciélagos pertenecientes a las especies Desmodus rotundus y Tadarida brasiliensis de Uruguay. Tesis de grado, Universidad de la República. https://www.colibri.udelar.edu.uy/items/f08d1df4-1f48-465f-9c00-1c9fcd95d50b

[20] Paridaen, J.T. and Huttner, W.B. (2014) Neurogenesis during Development of the Vertebrate Central Nervous System. *The EMBO Reports*, **15**, 351-364. https://doi.org/10.1002/embr.201438447

[21] Malmierca, M.S. (2022) How the Bat Brain Detects Novel Sounds (Commentary on Wetekam *et al*., 2021). *European Journal of Neuroscience*, **55**, 895-897. https://doi.org/10.1111/ejn.15606

[22] Ulanovsky, N. and Moss, C.F. (2008) What the Bat's Voice Tells the Bat's Brain. *Proceedings of the National Academy of Sciences*, **105**, 8491-8498. https://doi.org/10.1073/pnas.0703550105

[23] Kishida, R., Goris, R.C., Terashima, S. and Dubbeldam, J.L. (1984) A Suspected Infrared-Recipient Nucleus in the Brainstem of the Vampire Bat, Desmodus Rotundus. *Brain Research*, **322**, 351-355. https://doi.org/10.1016/0006-8993(84)90132-x

[24] Rampelotto, P.H., Giannakos, N.R.O., Mena Canata, D.A., Pereira, F.D., Hackenhaar, F.S., Pereira, M.J.R., *et al*. (2023) Oxidative Stress and Antioxidant Defense in the Brain of Bat Species with Different Feeding Habits. *International Journal of Molecular Sciences*, **24**, Article 12162. https://doi.org/10.3390/ijms241512162

[25] Smith, T.D. and Bhatnagar, K.P. (2019) Anatomy of the Olfactory System. In: Doty, R.L., Ed., *Handbook of Clinical Neurology*: *Smell and Taste*, Vol. 164, Elsevier, 17-28.

[26] Palacios Prü, E.L. and Mendoza Briceño, R.V. (1972) An Unusual Relationship between Glial Cells and Neuronal Dendrites in Olfactory Bulbs of Desmodus Rotundus. *Brain Research*, **36**, 404-408. https://doi.org/10.1016/0006-8993(72)90744-5

[27] De Saint Jan, D. and Westbrook, G.L. (2005) Detecting Activity in Olfactory Bulb Glomeruli with Astrocyte Recording. *The Journal of Neuroscience*, **25**, 2917-2924. https://doi.org/10.1523/jneurosci.5042-04.2005

[28] Heuer, K., Traut, N., de Sousa, A.A., Valk, S.L., Clavel, J. and Toro, R. (2023) Diversity and Evolution of Cerebellar Folding in Mammals. *eLife*, **12**, e85907.

[29] Washington, S.D., Hamaide, J., Jeurissen, B., van Steenkiste, G., Huysmans, T., Sijbers, J., *et al*. (2018) A Three-Dimensional Digital Neurological Atlas of the Mustached Bat (Pteronotus Parnellii). *NeuroImage*, **183**, 300-313. https://doi.org/10.1016/j.neuroimage.2018.08.013

[30] Simmons, A.M., Warnecke, M. and Simmons, J.A. (2024) Microseconds-Level Coding of Echo Delay in the Auditory Brainstem of an FM-Echolocating Bat. *Journal of Neurophysiology*, **132**, 2012-2022. https://doi.org/10.1152/jn.00305.2024

[31] Bhatnagar, K.P. (1988) Ultrastructure of the Pineal Body of the Common Vampire Bat, *Desmodus rotundus*. *American Journal of Anatomy*, **181**, 163-178. https://doi.org/10.1002/aja.1001810206

[32] Schnell, S. and Maher de Leon, M.E. (1998) Anatomy of the Central Nervous System. *Seminars in Oncology Nursing*, **14**, 2-7. https://doi.org/10.1016/s0749-2081(98)80037-5

[33] Allen Institute for Brain Science (2008) Allen Mouse Spinal Cord Atlas: Reference Sets [Atlas de referencia/Conjunto de datos]. Allen Brain Map. https://mousespinal.brain-map.org/imageseries/showref.html

[34] Radtke-Schuller, S., Fenzl, T., Peremans, H., Schuller, G. and Firzlaff, U. (2020) Cyto- and Myeloarchitectural Brain Atlas of the Pale Spear-Nosed Bat (*Phyllostomus discolor*) in CT Aided Stereotaxic Coordinates. *Brain Structure and Function*, **225**, 2509-2520. https://doi.org/10.1007/s00429-020-02138-y

[35] Garman, R.H. (2011) Histology of the Central Nervous System. *Toxicologic Pathology*, **39**, 22-35. https://doi.org/10.1177/0192623310389621

[36] Arendt, D., Denes, A.S., Jékely, G. and Tessmar-Raible, K. (2008) The Evolution of Nervous System Centralization. *Philosophical Transactions of the Royal Society B: Biological Sciences*, **363**, 1523-1528. https://doi.org/10.1098/rstb.2007.2242

[37] Vita, M. and Álvarez, F.G. (2026) Anatomía del cerebro y las meninges. In: Zuccolilli, G.O., Ed., *Neuroanatomía y neurofisiología animal: Conceptos básicos para medicina veterinaria*, Editorial de la Universidad Nacional de La Plata, 221-264. https://sedici.unlp.edu.ar/handle/10915/196091

[38] Coy Moreno, L.Y. (2016) Estrategia didáctica para el aprendizaje de la histología del sistema nervioso. Trabajo Final de Maestría, Universidad Nacional de Colombia.

[39] Ramírez Muñoz, M.G. (2025) Estudio morfológico comparativo del hipotálamo y la hipófisis y construcción de un modelo 3-D en los murciélagos hematófagos *Desmodus rotundus* y *Diphylla ecaudata*. Tesis de Maestría, Universidad Autónoma del Estado de Hidalgo.